EAN 2024 62th annual conference on experimental stress analysis

Determination of the Dynamic Bending and Torsional Stiffness of a Beam using Enhanced FRF

R. Huňady [1,a], P. Palička [1], E. Dubňanská [1], M. Hančinová [1]

[1] *Technical University of Košice, Faculty of Mechanical Engineering, Letná 1/9, Košice, Slovakia*
[a] *robert.hunady@tuke.sk*

Abstract: This paper deals with the estimation of dynamic stiffness coefficients from the so-called enhanced frequency response functions (EFRFs), which are extracted from the FRF matrix obtained in the modal test. To determine the bending and torsional stiffness parameters, the synthesized EFRF obtained by the curve-fitting method is used. The given procedure is presented on the example of a free straight beam with a constant cross section.

Keywords: bending stiffness; torsional stiffness; estimation; modal analysis; EFRF.

1 Introduction

Determining the stiffness of components is a common issue in engineering practice. Most often, the tensile, flexural and torsional stiffness coefficients are determined as a structural response to static loads. For simple shaped components such as beams, shafts, etc., it is possible to find analytical formulas in the literature for the calculation of stiffness coefficients for various boundary conditions [1]. In the case of parts with complex geometry, they are determined using numerical simulations or experimental measurements. A typical practical application is vehicle body stiffness analysis to determine bending, torsional and lateral stiffness [2-5]. It is well known that these parameters have a significant influence on the comfort and driving characteristics of the car. Other examples could be found in civil engineering [6], or in the aerospace industry [7, 8]. Unlike static stiffness, dynamic stiffness exhibits different values depending on the rate of object deformation or the frequency of vibration. The dynamic stiffness coefficient is defined as the frequency dependant ratio between the amplitude of the dynamic force and the amplitude of the dynamic displacement. Based on this, it is evident that an increase in dynamic stiffness will reduce the vibration response of the system and vice versa. The static data is contained in the dynamic data (at a frequency of 0 Hz). In the following section, it will be shown how an estimate of the stiffness coefficients can be obtained from the frequency characteristics of the structure.

To determine the dynamic stiffness coefficients, we can use the so-called Enhanced Frequency Response Functions (EFRF), which are the result of transforming the responses from physical to modal space. In this way, it is possible to isolate a selected mode and express it in terms of the response of a system with one degree of freedom. The enhanced frequency response function of an arbitrary *r*-th mode can be determined as follows [9]

$$EFRF(\omega)_r = \{U(\omega_r)\}^H [H(\omega)] \{V(\omega_r)\}, \tag{1}$$

where the mode shape vector $\{U(\omega_r)\}$ and the vector of modal participation factors $\{V(\omega_r)\}$ of the *r*-th mode serve as discrete modal filters that amplify the response of the *r*-th mode, while the responses of the other modes are attenuated. Vectors $\{U(\omega_r)\}$ and $\{V(\omega_r)\}$ are obtained by singular value decomposition (SVD) of the FRF matrix $[H(\omega)]$ done for each spectral line

$$[H(\omega)] = [U(\omega)]^H [S(\omega)][V(\omega)], \tag{2}$$

where $[S(\omega)]$ is a diagonal singular value matrix. The plot of singular values corresponds to the Complex Mode Indicator Function (CMIF)

$$CMIF(\omega)_k = S_k(\omega)\,. \tag{3}$$

If we extract the EFRF functions for the first bending and first torsional modes in this way, then the dynamic stiffness coefficient can be determined from the compliance line $\kappa(\omega)$ tangent to the left part of the EFRF curve (see Fig. 1). The tangent to the right part expresses the modal mass of the mode. Depending on the type of FRF, the compliance of the mode is given by

$$\kappa(\omega) = \frac{1}{k} \text{ - for receptance,} \quad \kappa(\omega) = \frac{\mathrm{i}\omega}{k} \text{ - for mobility,} \quad \kappa(\omega) = \frac{-\omega^2}{k} \text{ - for inertance.} \tag{4}$$

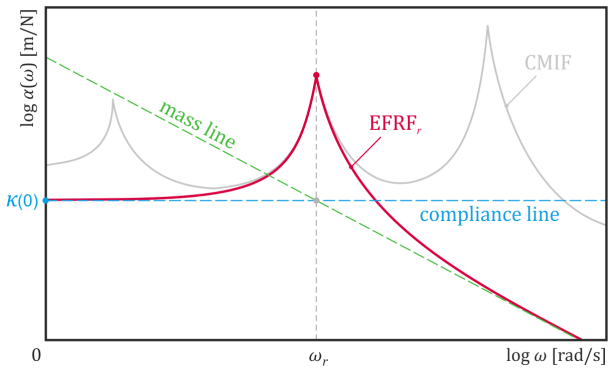

Fig. 1: Isolated response of the selected mode in the form of a receptance.

The detailed procedure for deriving the compliance curve and calculating the stiffness coefficients is given in Chapter 3.

2 Experimental Modal Analysis a Free-free Beam

The object of the modal test was a steel beam of rectangular cross-section with dimensions 40x8x400 mm. The beam was loaded quasi-freely using two rubber bands (Fig. 2a). A B&K impact hammer Type 8206 was used for excitation. The responses were measured using a Polytec PDV100 laser vibrometer. The geometric model (Fig. 2b) consisted of 18 input DOFs and 1 output DOF. The measurements were evaluated in the Pulse Reflex software. In the frequency range up to 6000 Hz, 9 modes were identified. The first bending and the first torsional mode shape of the beam with the modal parameters are shown in Fig. 3.

a)  b) 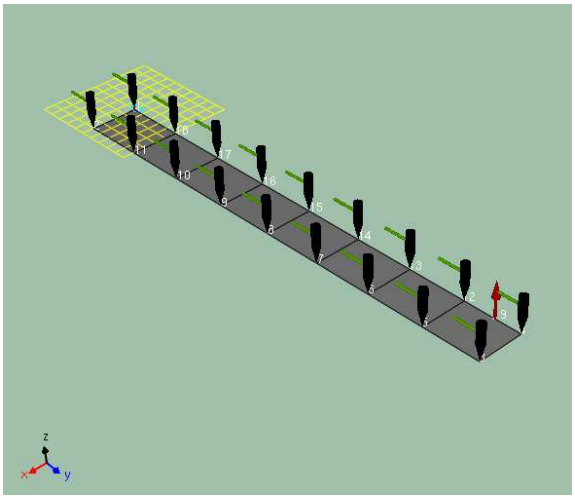

Fig. 2: a) measurement of modal parameters, b) geometric model.

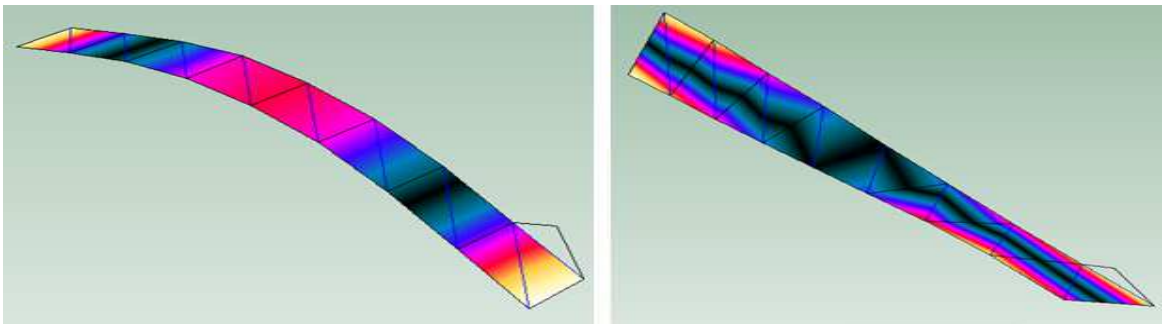

Fig. 3: The 1. bending (f_1 = 266.5 Hz, ζ_1 = 0.00386) and the 1. torsional mode (f_4 = 1496.8 Hz, ζ_4 = 0.00163).

3 Estimation of Stiffness Coefficients

All frequency response functions (FRFs) obtained from the measurements were exported to MATLAB for further processing. In the first step, they have been converted from mobility $Y(\omega)$ to receptance $\alpha(\omega)$ according to the well-known relation

$$\alpha(\omega) = \frac{Y(\omega)}{\mathrm{i}\omega}\,. \tag{5}$$

Subsequently, the FRF matrix was constructed and based on the procedure described in Chapter 1, the CMIF and EFRF functions were extracted (see Fig. 4). As can be seen in the figure, the EFRF curves do not exactly correspond to the ideal response of a SDOF system. This shortcoming is due to the limited number of data in the eigenvectors that are used as modal filters. Nevertheless, the frequency response in the vicinity of the natural frequency is sufficiently isolated from the other modes and can be used to construct a synthesized EFRF.

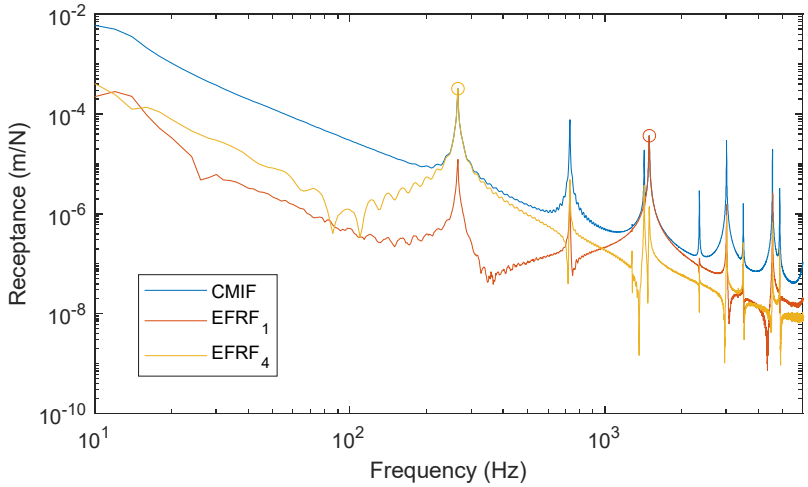

Fig. 4: CMIF and EFRF plot of the first bending and the first torsional mode.

Since the response of an arbitrary mode is most dominant around its resonant frequency, the so-called spectral bell was first defined. This bell is represented by a small region of the resonant peak. Basically, it consists of a small number of data, as can be seen in Fig. 5. The synthesized EFRF was determined using the curve fitting method, starting from the equation

$$EFRF(\omega)_{synt,r} = \frac{Q_r}{\lambda_r - \omega^2}\,, \tag{6}$$

where Q_r is the modal scale factor, $\lambda_r = \Omega_r^2\left(1 + \mathrm{i}\frac{\zeta_r}{2}\right)$ is the complex pole, Ω_r is the natural angular frequency, and ζ_r is the damping of the r-th mode.

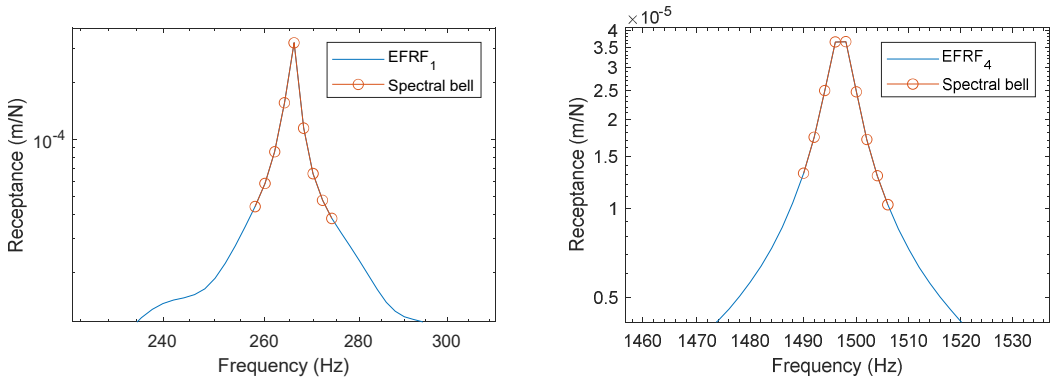

Fig. 5: Spectral bell defined on EFRF curve.

MATLAB optimization tools were used to determine the three unknown parameters Q_r, Ω_r, and ζ_r. The objective function was to minimize the differences between the measured and synthesized EFRF on the frequency band ω_{sb} of the spectral bell of the corresponding mode

$$\min\left(\left\|EFRF(\omega_{sb})_{exp,r} - EFRF(\omega_{sb})_{synt,r}\right\|\right). \tag{7}$$

The modal parameters (f_r, ζ_r) extracted from the measurements were used as initial values of the design variables. The initial estimate of the modal scale factor was determined as follows

$$Q_r = 2\, EFRF(\Omega_r)\, \Omega_r^2\, \zeta_r, \tag{8}$$

where $\Omega_r = 2\pi f_r$. The `fminsearch` function, which searches for the minimum of an unconstrained multivariate function using a derivative-free method, was used for the computation. The optimized values of the search variables are shown in Tab. 1. Fig. 6 and Fig. 7 show the resultant synthesized EFRF plot of the first bending and the first torsional mode, respectively.

Tab. 1: Modal parameters obtained in the curve-fitting process.

Mode	Q_1 ($\mathrm{Nm^{-1}s^{-2}}$)	f_1 (Hz)	ζ_1 (–)	Mode	Q_4 ($\mathrm{Nm^{-1}s^{-2}}$)	f_4 (Hz)	ζ_4 (–)
bending	6.272669	265.66	0.003265	torsional	11.356699	1496.98	0.001622

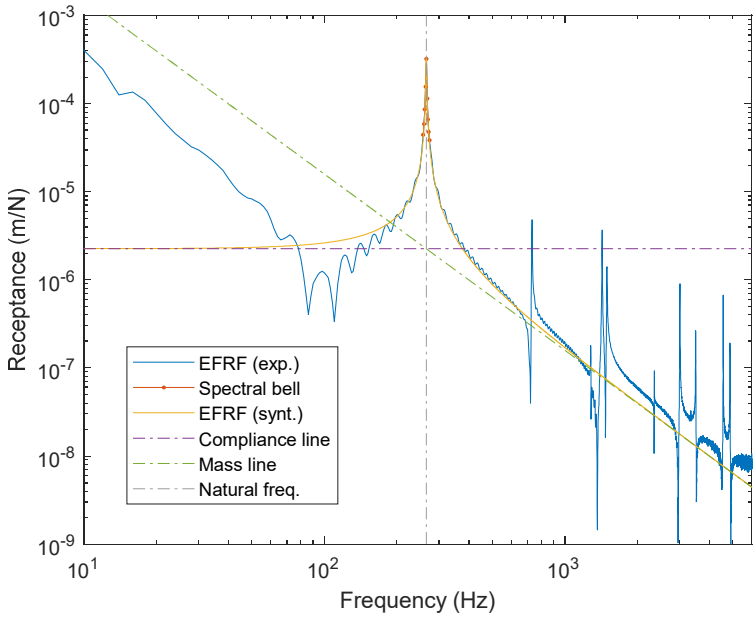

Fig. 6: EFRF of the first bending mode.

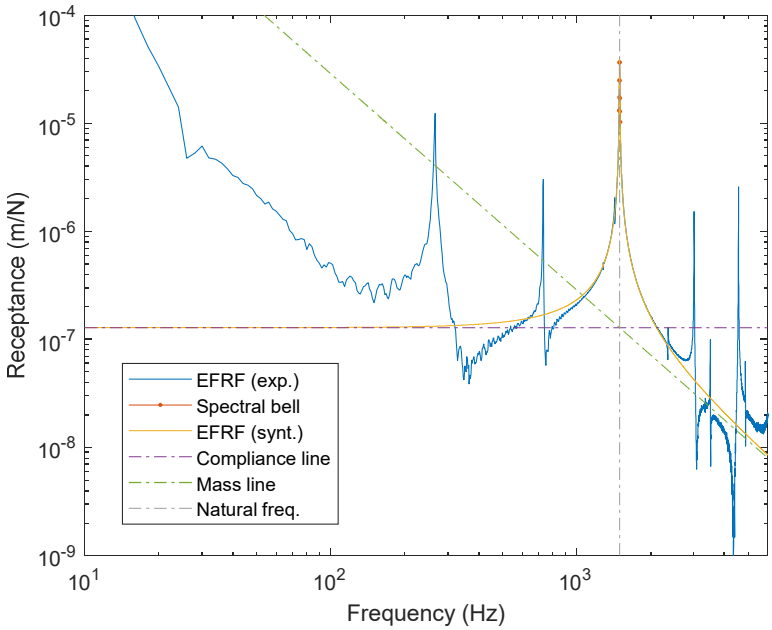

Fig. 7: EFRF of the first torsional mode.

Since the spectra shown in Fig. 6 and Fig. 7 represent the receptance, i.e. the mechanical compliance (m/N), the stiffness is given as the inverse value. For a free-free beam, the bending stiffness coefficient k_b is determined as

$$k_b = \frac{1}{2\kappa(0)}, \tag{9}$$

where $\kappa(0)$ is the compliance value at zero frequency taken from the synthesized EFRF. To calculate the torsional stiffness coefficient k_t of the beam, it is necessary to use the equation

$$k_t = \frac{b^2}{4\kappa(0)}, \tag{10}$$

where b is the beam width. Equation (10) converts the value of the stiffness coefficient from N/m to Nm/rad. The resultant coefficients are listed in Tab. 2.

Tab. 2: Dynamic bending and torsional stiffness coefficients of a free-free beam.

Mode	$\kappa(0)$	k_b (N/m)	Mode	$\kappa(0)$	k_t (Nm/rad)
1. bending	$1.9532 \cdot 10^{-6}$	255990	1. torsional	$1.19424 \cdot 10^{-7}$	3349

4 Conclusion

The aim of the paper was to present an alternative approach for determining the stiffness parameters of the structure. Using the example of a free beam, it was shown how the dynamic stiffness coefficients in bending and torsion can be determined from the frequency response functions. The key is to isolate the frequency response of the corresponding mode, for which the enhanced frequency response function can be advantageously used. As has been shown the degree of isolation depends on the eigenvectors, which means that increasing the number of DOFs of the geometric model can lead to better estimation.

Acknowledgement

This work was supported by the Science Grant Agency of the Ministry of Education, Science, Research and Sport of the Slovak Republic and the Slovak Academy of Sciences under the project VEGA 1/0324/24.

References

[1] F. Trebuňa, F. Šimčák, Resistance of Elements of Mechanical Systems, 1. ed., Technical University of Košice, Košice, 2004. (in Slovak)

[2] L. Shengqin, F. Xinyuan, Study of structural optimization design on a certain vehicle body-in-white based on static performance and modal analysis, Mechanical Systems and Signal Processing 135 (2020) 106405, https://doi.org/10.1016/j.ymssp.2019.106405.

[3] D. Mundo, R. Hadjit, S. Donders, M. Brughmans et al., Simplified modelling of joints and beam-like structures for BIW optimization in a concept phase of the vehicle design process, Finite Elements in Analysis and Design 45(6) (2009) 456–46, https://doi.org/10.1016/j.finel.2008.12.003.

[4] A. Ramachandran, H. Reddy, T. Chavali, A. Hukar et al., Body-in-White Joint Stiffness Sensitivity Analysis, SAE Technical Paper (2019) 2019-01-5012, https://doi.org/10.4271/2019-01-5012.

[5] S.Y.R. Aizzat, R. Rahizar, M.H. Sallehuddin, A. Anuar, Improving the Dynamic Characteristics of Body-in-White Structure Using Structural Optimization, The Scientific World Journal 2014 (2014) 190214, https://doi.org/10.1155/2014/190214.

[6] L. Xiang, T. Shitan, Z. Xueyi, L. Xiao et al., Dynamic response analysis for bridges subjected to moving vehicle loads by using the analytical dynamic stiffness method, Computers & Structures 292 (2024) 107240, https://doi.org/10.1016/j.compstruc.2023.107240.

[7] S. Qiao, J. Jiao, Y. Ni, H. Chen, X. Liu, Effect of Stiffness on Flutter of Composite Wings with High Aspect Ratio, Mathematical Problems in Engineering 2021 (2021) 6683032, https://doi.org/10.1155/2021/6683032.

[8] Q. Ming, Z. Wenguo, L. Shu, The Effect of Torsional and Bending Stiffness on the Aerodynamic Performance of Flapping Wing. Aerospace 10(12) (2023) 1035, https://doi.org/10.3390/aerospace10121035.

[9] R.J. Allemang, D.L. Brown, A complete review of the complex mode indicator function (CMIF) with applications, in proc.: International Conference on Noise and Vibration Engineering (ISMA) (2006), Katholieke Universiteit Leuven, Belgium, 3209–3246.